Journal of Rock Mechanics and Geotechnical Engineering 8 (2016) 50–59

Contents lists available at ScienceDirect

Journal of Rock Mechanics and Geotechnical Engineering

journal homepage: www.rockgeotech.org

Full length article

Carbon sequestration potential of the Habanero reservoir when carbon dioxide is used as the heat exchange fluid

Chaoshui Xu [a,*], Peter Dowd [a], Qi Li [b]

[a] School of Civil, Environmental and Mining Engineering & South Australia Centre for Geothermal Energy Research, University of Adelaide, Adelaide, 5005, Australia

[b] State Key Laboratory of Geomechanics and Geotechnical Engineering, Institute of Rock and Soil Mechanics, Chinese Academy of Sciences, Wuhan, 430071, China

ARTICLE INFO

Article history:
Received 4 March 2015
Received in revised form
27 April 2015
Accepted 8 May 2015
Available online 25 June 2015

Keywords:
Carbon sequestration
Carbon dioxide (CO_2) geological storage capacity
Enhanced geothermal system (EGS)
CO_2-EGS
Habanero project

ABSTRACT

The use of sequestered carbon dioxide (CO_2) as the heat exchange fluid in enhanced geothermal system (EGS) has significant potential to increase their productivity, contribute further to reducing carbon emissions and increase the economic viability of geothermal power generation. Coupled CO_2 sequestration and geothermal energy production from hot dry rock (HDR) EGS were first proposed 15 years ago but have yet to be practically implemented. This paper reviews some of the issues in assessing these systems with particular focus on the power generation and CO_2 sequestration capacity. The Habanero geothermal field in the Cooper Basin of South Australia is assessed for its potential CO_2 storage capacity if supercritical CO_2 is used as the working fluid for heat extraction. The analysis suggests that the major CO_2 sequestration mechanisms are the storage in the fracture-stimulation damaged zone followed by diffusion into the pores within the rock matrix. The assessment indicates that 5% of working fluid loss commonly suggested as the storage capacity might be an over-estimate of the long-term CO_2 sequestration capacity of EGS in which supercritical CO_2 is used as the circulation fluid.

1. Introduction

It is widely accepted that anthropogenic carbon dioxide (CO_2) emissions into the atmosphere is one of the major causes of global warming (Metz et al., 2005). Although the ultimate solution is to move away from our dependency on fossil fuels, it is unlikely that this dependency will be eliminated in the near future. Various techniques have been explored to capture and store emitted CO_2 including natural sequestration of CO_2 in plants and carbon in soil and the storage of CO_2 in geological reservoirs or geological sequestration (Huisingh et al., 2015).

Broadly speaking, geological storage refers to any method that results in the permanent storage of CO_2 beneath the surface of the Earth. This could include injection of CO_2 underground purely for the purpose of storage (e.g. in a depleted oil or gas field) or the use of CO_2 as a working fluid to assist/enhance industrial production whilst simultaneously achieving the permanent storage of CO_2. Over the past decade or so much research has focused on the latter category because of the additional financial benefit, which makes it more likely that large-scale commercial operations will be established using techniques in this category (Xie et al., 2014).

Most of the work in the use of CO_2 to assist/enhance production has been in CO_2 enhanced oil recovery (CO_2-EOR), CO_2 enhanced gas recovery (CO_2-EGR), CO_2 enhanced coal-bed methane recovery (CO_2-ECBM), CO_2 enhanced shale gas recovery (CO_2-ESGR), CO_2 enhanced geothermal system (CO_2-EGS), CO_2 enhanced uranium leaching (CO_2-EUL), and CO_2 enhanced saline water recovery (CO_2-EWR) (Li et al., 2015a). A detailed discussion of these techniques was documented in ACCA21 (2014). Of these techniques, CO_2-EOR is perhaps the most developed and there are many commercial operations in Canada, China and USA (Manrique et al., 2010; ACCA21, 2014; Lv et al., 2015). The other techniques are still mainly in the development stage although research has, to date, demonstrated their significant potential (ACCA21, 2014; Li et al., 2015b).

CO_2 has different phases and it readily becomes a supercritical fluid ($scCO_2$) as it reaches its critical point at a temperature of 31.1 °C and a pressure of 7.38 MPa. In its supercritical state, CO_2 has some desirable properties that make it very useful in a wide range of industrial applications. For example, the density (ρ) of $scCO_2$ is a little less than that of water but it has a much lower viscosity (μ, ρ/μ of $scCO_2$ is about 1.7 times that of water at a temperature of 200 °C),

* Corresponding author. Tel.: +61 400800933.
E-mail address: chaoshui.xu@adelaide.edu.au (C. Xu).

Peer review under responsibility of Institute of Rock and Soil Mechanics, Chinese Academy of Sciences.
1674-7755
http://dx.doi.org/10.1016/j.jrmge.2015.05.003

higher compressibility and expandability (i.e. higher expansion coefficient), and a surface tension of almost zero. These properties make it much easier for $scCO_2$ to flow within pores or fractures in rock masses and make $scCO_2$ almost an ideal working fluid for reservoir fracture stimulation, pressure expulsion (e.g. for EOR, EGR, ESGR, EWR) or fluid circulation (e.g. for EGS). The $scCO_2$ is also a strong extraction solvent for heavy oil or other organic matter and, when mixed with oil, it reduces significantly the viscosity and density of oil and therefore can enhance significantly the recovery rate (EOR). The high compressibility and expandability of $scCO_2$ make it easier to maintain a high buoyancy force within the reservoir so as to enhance the production rate (EGS, EOR, EGR). For CO_2-EGS, $scCO_2$ has the added advantage of reducing scaling in both the reservoir and the circulation system, which is a serious problem in geothermal applications. The $scCO_2$ is much less likely to dissolve in-situ minerals compared with the highly corrosive brine normally encountered in EGS reservoirs. During the process of enhancing production, $scCO_2$ will dissipate from the injection well, become trapped within the pores or fractures in rock masses, react with other minerals or dissolve in water and hence achieve permanent geological storage.

This paper assesses the CO_2 storage capacity for CO_2-EGS, taking the Habanero reservoir as an example. In EGS, the working fluid normally considered is water (or brine). Brown (2000) was the first to suggest the use of $scCO_2$ as a working fluid for EGS. He identified three major advantages of using $scCO_2$ instead of water as the working fluid taking the Fenton Hill reservoir as an example: (1) the buoyancy force is equivalent to adding an additional 22 MPa of pressure difference between the injection and production wells and hence increases the mass production rate significantly; (2) as it does not dissolve minerals in the reservoir, its use could potentially eliminate the scaling problem in the system; (3) hot dry rock (HDR) reservoirs with temperatures in excess of the critical temperature for water (374 °C) could be developed without the problems associated with dissolving silica, which could increase the thermodynamic efficiency of surface power-conversion units. Brown (2000) also noted that the low heat capacity of $scCO_2$ (40% of the heat capacity of water) is an unfavourable property as the heat that can be absorbed per unit weight of $scCO_2$ is lower than that of water. Although no modelling work was done, Brown suggested that, after taking into account the additional production rate and the higher buoyancy force (hence less power is needed to drive the fluid circulation), a CO_2-EGS should produce approximately the same power as a water-based system if all other conditions are equal.

EGS reservoirs are pressurised in the heat production process. The higher pressure within the reservoir compared with its surroundings will force the fluid to diffuse into the surrounding rock masses through faults, fractures and pores. In general, this fluid loss is not recoverable unless the reservoir is negatively pressured for a long period of time. It is, therefore, possible to achieve permanent storage of CO_2 in this application if $scCO_2$ is used as the working fluid. EGS are normally created in geological formations with very low permeability, either within the crystalline rock or in the sedimentary layer directly above the basement rock (heat source). In this case, the reservoir must be stimulated to create fracture networks and hence a permeable reservoir with a permeability suitable for heat production. Within this context, the estimation of CO_2 storage capacity for a given stimulated reservoir and operating scenario is important in optimising the design not only for energy production, but also for the required storage capacity. In the work by Brown (2000), a figure of 0.3 kg/s ($\sim$9460 t/a) of CO_2 per 1 MW of electric power generated was given as a prediction for the sequestration capacity of EGS reservoirs, although no detail was given on how this figure was obtained.

2. Enhanced geothermal systems (EGS)

EGS have the potential to provide substantial amount of renewable energy due to the vast extent of the heat resources throughout the world (MIT, 2006; Xie et al., 2014). These resources, however, are in general located at significant depths (3–5 km below the surface) within geological formations of low permeability. For example, although crystalline rocks have significant radiogenic heat, their permeability is at the micro-Darcy or even nano-Darcy scale (Selvadurai et al., 2005; Bear and Cheng, 2010; Bundschuh and Suárez-Arriaga, 2010). The permeability of sedimentary rocks overlaying radiogenic heat sources is generally higher but at the milli-Darcy scale or less (Bundschuh and Suárez-Arriaga, 2010). Direct circulation of flow through these types of rocks for heat mining is obviously difficult if not impossible and requires the additional step of fracture stimulation to create fracture networks within the reservoir, hence the term EGS is used to describe these types of (enhanced) reservoirs. The fracture network generated by the stimulation should connect the injection and production wells to form significant flow pathways for the geothermal fluid. The permeability of open (stimulated) fractures is generally several magnitudes greater than that of the rock matrix and thus stimulation is expected to increase the permeability of the reservoir by several orders of magnitude. This level of increase in permeability is crucial for creating technically and commercially viable geothermal reservoirs. For commercial viability, an EGS reservoir should be able to achieve a flow rate of at least 100 L/s.

The depth and re-engineering of the reservoir impose many significant technical challenges for the commercial exploitation of EGS. The outcomes from major EGS projects around the world over the past 40 years are very mixed (Tenzer, 2001). The world's first EGS project, starting in the early 1970s, was at Los Alamos in New Mexico and was successful in the sense that it proved the concept by achieving flow circulation between injection and production wells through the stimulated fractures. The Phase II system produced 4–6 MW of geothermal power by circulating the fluid at a rate of approximately 6 L/s at an injection pressure of around 27 MPa. The project stopped in 1995 mainly due to budget shortfalls (Duchane and Brown, 2002; Brown et al., 2012). The Rosemanowes project in the UK achieved a production rate of 16.7 L/s at an injection pressure of 10 MPa with a three-well configuration during its Phase 2C stage, but the project was terminated in 1991 following the inability to seal the reservoir during the Phase 3 stimulation (Parker, 1999). The Ogachi HDR project in Japan achieved a low circulation rate of about 2 kg/s at a wellhead pressure of 13 MPa with a two-well configuration after multiple stimulations of the two wells. The project was stopped in 2002 for financial reasons (Kaieda et al., 2005). The Hijiori project in Japan suffered a similar fate and the project was stopped in 2002 despite having established a circulation between a four-well system with a production rate of 6.7 kg/s at an injection pressure of 8.1 MPa (Oikawa et al., 2001; Matsunaga et al., 2005). The European Community Soultz-sous-Forêt HDR project in France continues to operate. The pilot electricity plant was constructed in 2007 with a capacity of 1.5 MW and the latest published figures (for 2011) report a production rate of 23–26 L/s and a net electrical power of 100 kW was produced. The thermal power produced was 8474 kW and the gross power produced was 655 kW, suggesting a utilisation efficiency of around 7.8% (Albert et al., 2012). This project has taken more than 20 years and significant investments from the European Union to bring it to this stage. The project is regarded as an R&D project at this stage as it is still not commercially viable, although it does demonstrate the potential of HDR EGS. Geodynamics' Cooper Basin project in South Australia was started in 2002 (Weidler, 2005; Baisch et al., 2006). Four wells were drilled and the final Habanero 4 (H4) well was

completed in 2012. Following investments of almost nearly 200 million US dollars, the pilot plant was established using Habanero 1 (H1) as the injection well and H4 as the production well. The trial was successful and Geodynamics is now evaluating the commercial potential of the project. On a smaller scale, the Landau plant in Germany, with a flow rate of 80 L/s and thermal power of 3 MW, has been running successfully since 2007 and the possibility of expansion is under investigation (BESTEC, 2012). Although Landau is a combined EGS and hydrothermal plant, it is the first commercially viable project using EGS technology. The total investment was 3.6 million US dollars and it is estimated that income will have repaid the capital sometime in 2017.

Clearly there is still some ways to go for EGS to become an accepted, commercially viable, sustainable energy production technique. Nevertheless, a great deal of progress has been made since the Fenton Hill project. Significant knowledge and experience have been accumulated in terms of site selection, fracture stimulation, well design and completions, and power plant design. This expertise will benefit future projects, particularly the new projects planned in countries such as China, Korea, USA and some European countries.

3. Habanero geothermal reservoir

The Geodynamics Habanero reservoir in the Cooper Basin of South Australia is the first HDR heat resource in Australia to be exploited for geothermal energy. The first well, H1, was drilled in 2003 to a depth of 4421 m, 753 m into the granite basement rock. The bottom 282 m section is a 6-inch open-hole section and the rest of the well is cased. The highest temperature recorded was 248.3 °C at 4391 m, 30 m above the total depth, which suggests a likely bottom hole temperature in excess of 250 °C. Prior to the fracture stimulation, a series of injection tests was conducted which indicated the injectivity of the natural reservoir to be around 1 L/(MPa s). The injection tests also indicated a baseline reservoir pressure of approximately 35 MPa above hydrostatic which confirms that the Habanero granite is a confined reservoir tightly sealed from the overlaying sediments with unknown but finite volume.

The hydraulic fracture stimulation of the reservoir was done by a fracture initiation phase followed by two main stimulation stages. A total volume of 1700 m^3 of water was injected during the fracture initiation phase, which was designed to open up multiple fractures to maximise the effects of subsequent fracture stimulation phases. In the first major fracture stimulation stage, a total of 13,000 m^3 of water was injected over a period of about 11 days. The second main fracture stimulation was done through casing perforations between depths of 3993 m and 4137 m and the total volume of water injected was 3000 m^3. During these injections, the peak wellhead pressure was 69 MPa and the peak injection rate was 63 L/s. More details of the well completion and the fracture stimulation processes can be found in Weidler (2005).

H1 was designed to be the injection well of the future pilot plant. Based on the seismic event cloud obtained from the fracture stimulations, the designed production well, Habanero 2 (H2), was drilled in 2004 about 500 m southwest of H1. H2 intersected the first permeable zone in the granite at 4181 m and a highly stimulated zone at 4325 m, 15 m below the depth predicted by the seismic analysis. The pressure responses in H1 to mud pumping cycles in H2 clearly demonstrated the hydraulic connectivity between the two wells. Unfortunately, a collar failure occurred during subsequent drilling and about 245 m of the drill string was lost. A side-track was drilled to complete the well to a depth of 4358 m. The side-track intersected the two major permeable zones mentioned above at approximately the same depth (4185 m and 4330 m, respectively). H2 was hydraulically stimulated in 2005 with 3800 m^3 of water injected. Following this stimulation, H1 was re-stimulated with a total volume of 17,000 m^3 of water injected. Accordingly, the injectivity of H1 increased to approximately 1.6 L/(MPa s). However, a blockage in H2 in 2005 resulted in the loss of the well despite various attempts to pass by the blockage.

Habanero 3 (H3), with a larger diameter of 8.5 inch at the bottom of the well, was drilled in 2007 and completed in 2008, about 560 m northeast of H1. The well was completed at a depth of 4221 m and a temperature of 244 °C was recorded at a depth of 4180 m. The well was stimulated in 2008 with 2200 m^3 of water injected to achieve an injectivity of approximately 2 L/(MPa s). A short-term open-flow circulation test between H1 and H3 in 2008 achieved a flow rate of 18.5 kg/s with a temperature of ~212.5 °C at an injection pressure of 50.8 MPa. This was followed by a period of closed-loop flow testing between the two wells which achieved a flow rate of 15.6 kg/s with a temperature of ~212.5 °C and an outlet pressure of 44.8 MPa. A tracer test was also conducted yielding a breakthrough time of 4 days and a peak return time of 9 days. The mean residence time was 23.7 days and 78% of the tracer added was recovered. However, a casing failure near the surface in 2009 led to the decision on pluging and capping the well.

H4, about 145 m east-northeast of H3 (690 m from H1), also with a 8.5 inch well design, was drilled in 2012 to the depth of 4225 m. The injectivity of H4 was about 4.5 L/(MPa s) during a local fracture stimulation conducted in October 2012 when 2500 m^3 of water was injected. An extended stimulation over the following month with 34,000 m^3 of water injected significantly improved the injectivity to a maximum of 16 L/(MPa s). All stimulations were carried out with a maximum surface pressure of 48.3 MPa. The open-flow testing achieved a maximum flow rate of 50 kg/s and the closed-loop circulation test in early 2013 between H1 and H4 achieved a maximum flow rate of 18.9 kg/s at the maximum temperature of 215 °C.

The 1 MW electricity generation pilot plant was commissioned in April 2013 and the trial run of the plant lasted for 160 days and concluded successfully in October 2013. Currently Geodynamics is exploring possible commercial exploitation of the geothermal field including a possible six well field development plan for a fluid production rate of 90–120 kg/s (Geodynamics, 2014).

As a summary for this section, Table 1 lists the figures discussed above related to the development of the Habanero geothermal field (Weidler, 2005; Wyborn, 2012; Geodynamics, 2014).

4. Habanero reservoir fracture model

During the fracture stimulation process, the surfaces of existing fractures can slip against each other due to the reduction in effective normal stress acting across the fractures; the misalignment of surface profiles results in dilation and hence increases the permeability of the fractures. New fractures can also be created during the stimulation process if the hydraulic pressure is high enough to overcome the minimum in-situ compressive stress. The Habanero basement rock is coarse-grained granite and pre-existing fractures are believed to be cemented with quartz; this belief is supported by core samples collected from other wells in the area. The estimated ratios of the principal stresses (σ_{hmax}:σ_{hmin}:σ_v) in the Habanero field are (1.35–1.45):(1.1–1.25):1 with the azimuth of σ_{hmax} being approximately 82°. Under this over-thrust stress regime, shallow dipping pre-existing fractures will be critically stressed and can be stimulated with hydraulic pressure much lower than the vertical overburden stress σ_v. For these reasons, it is believed that the Habanero stimulations are mainly shear slip in nature with some slips estimated to be in the order of centimetres based on the magnitude of the seismicity (Geodynamics, 2014).

Table 1
Summary of the development of the Habanero geothermal field.

Well	Depth (m)	Completion	Bottom hole temperature (°C)	Stimulation	Volume of water injected (m^3)	Injectivity (L MPa^{-1} s^{-1})	Number of seismic events	Note
H1	4421	2003	~250	2003	17,700	1	28,000	
				2005	17,000	1.6	17,000	
H2	4358	2005		2005	3800			Lost in 2005
H3	4221	2008	~245	2008	2200	2		Casing failure in 2009
H4	4225	2012		2012	2500	4.5	27,000	
					34,000	16		

Slip between fracture surfaces or fracture initiation/propagation will produce micro-seismicity that can be detected by an array of geophones, from which the locations of events can be determined. It is then reasonable to assume that at least one fracture passes through any seismic event point, which provides a very useful means of conditioning fracture models to give more realistic models of the stimulated reservoir. Seven major hydraulic stimulations were conducted over a period of about ten years with a total of approximately 80,000 m^3 of water injected, as discussed above. The three most significant stimulations were the H1 stimulation in 2003, H1 re-stimulation in 2005, and the H4 stimulation in 2012. During the 2003 stimulation, more than 28,000 seismic events were detected with over 22,000 of them successfully located by seismic signal analysis. The seismicity magnitudes could not be reliably determined from the geophones but the permanent seismometer network operated by Geoscience Australia recorded some events with magnitudes between 2.5 and 3.7. In 2005, more than 17,000 events were detected but only about 7000 were successfully located and the Geoscience Australia network detected only three events with magnitudes between 2.5 and 3. The 2012 stimulation produced 27,000 detected events with over 20,000 successfully located and the maximum magnitude was 3. The growth of the seismic cloud from the 2012 stimulation is consistent with the 2003 stimulation and together they cover a wider area of over 4 km^2 of the geothermal field, compared with approximately 2.5 km^2 obtained in the 2003 stimulation. The vertical extent of the seismic event cloud is approximately 500 m.

Here we use the seismic event cloud from the first major stimulation to demonstrate the fitting of a realistic conditional fracture model. In this case, eight geophones deployed in wells surrounding H1 at depths ranging from 100 m to 2300 m were used to record the seismic events generated by the stimulation process. A total number of 23,232 seismic events were successfully located and their absolute hypocentres are shown in Fig. 1. Note that in this paper we do not deal with the accuracy of the derived hypocentres.

Under the assumption that at least one fracture passes through each detected seismic point, it is possible, at least theoretically, to fit curved surfaces passing exactly through all seismic points but such a solution soon becomes impossible to be obtained in practice when the number of seismic points is significant and the fracture network is complex, as is the case for the Habanero reservoir. A compromise is to adopt the common approach in stochastic fracture modelling of using planar surfaces to represent fractures. As real fracture surfaces are tortuous, these planar surfaces can be considered as approximate first order representations in three-dimensional space. A fracture model thus constructed can be viewed as a first order representation of the reservoir that preserves all major features of the reservoir such as fracture connectivity and flow characteristics, which are important for the fluid flow and heat extraction analysis of the reservoir.

For such a first order approximation, the distance between the true but unknown curved fracture surface and the fitted planar surface, which can be approximately evaluated by the distances of the seismic points associated with the fracture to the fitted planar fracture, can then be used to assess the goodness-of-fit of the fracture model. Consider the fracture model (network) as a series of connected fracture planes, F_i ($i = 1, 2, \ldots, n$), where n is the total number of fractures, a seismic event point, P_j (j=1, 2,…, m) (where m is the total number of seismic event points) can then be associated with a fracture F_i with the distance of $d_{j:i}$. Because of the first order approximation of the fracture model, the complete set of projection distances $= \{d_{j:i}\}$, and j will exhibit random variation from the fitted fracture planes. A Gaussian model is the most appropriate statistical model to describe random variation, or noise, from a first order approximation, i.e. $d_{j:i} \sim N(0, \sigma^2)$ where σ^2 measures the degree of tortuosity of the fracture surfaces. The likelihood for the set of seismic event points $\boldsymbol{P}= \{P_j\}$, given a set of fitted fractures $\boldsymbol{F}= \{F_i\}$, can then be defined as

$$f(\{d_{j:i}\}) = \prod_{j=1}^{m} f(d_{j:i}|\boldsymbol{\theta}) = \left(\frac{1}{\sqrt{2\pi}\sigma}\right)^m \prod_{j=1}^{m} e^{-\frac{(d_{j:i})^2}{2\sigma^2}} \quad (1)$$

with the set of parameters $\boldsymbol{\theta} = \{x_i, y_i, z_i, \alpha_i, \beta_i, \gamma_i, a_i, b_i\}$ ($i = 1,2,\ldots,n$), where (x_i, y_i, z_i) are the coordinates of the centre of fracture plane i; (a_i, b_i) are the major and minor axes of the ellipse containing the fracture polygon; (α_i, β_i) are the dip direction and dip angle of the fracture plane; and γ_i is the rotation angle of the major axis of the ellipse against the dip direction of the fracture plane. The parameter space $\boldsymbol{\theta}$ is obviously significant and no direct solution is possible. One approach developed recently is to use Markov Chain Monte Carlo (MCMC) to sample the space $\boldsymbol{\theta}$ to derive a set of values of the constituent variables. Details can be found in Xu et al. (2013) and Mardia et al. (2007). Fig. 2 is a fracture model for the Habanero reservoir derived using this approach.

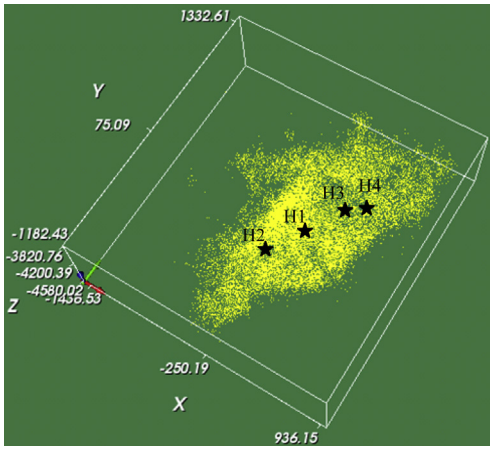

Fig. 1. Absolute hypocentre locations of the seismic events.

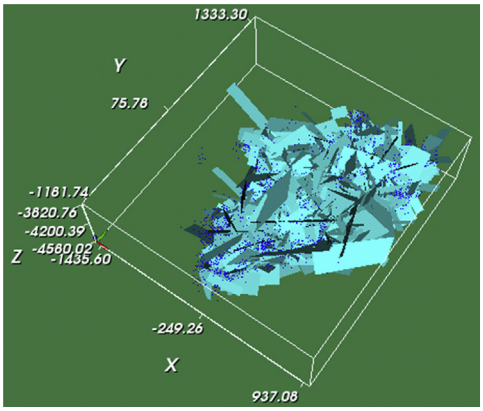

Fig. 2. Habanero fracture model derived by MCMC optimisation.

A more elegant approach developed more recently is the point and surface association consensus (PANSAC) approach (Xu and Dowd, 2014), which effectively fits a stochastic fracture propagation (SFP) model. The SFP model attempts to follow the fracture propagation sequence during the reservoir stimulation process and has been demonstrated to produce a model much closer to reality than models generated by other approaches based on assessments of reservoir characteristics (Xu and Dowd, 2014). Other recent approaches include the random sampling consensus (RANSAC) approach (Fadakar et al., 2013) and the clustering approach (Seifollahi et al., 2014a, b).

Fig. 3 shows a fracture model for the Habanero reservoir generated by the PANSAC algorithm. The model follows closely the gentle dipping (to southwest) feature of the seismic point cloud. A significant portion (42%) of the fractures has dip angles less than 30°, which is consistent with other analyses (Baisch et al., 2006). Based on the mud responses during the drilling of the Habanero wells, it is believed that there is a gentle dipping fault running across the reservoir. This fault was confirmed by the circumferential borehole imaging log (CBIL) of H3 which indicates a 5–6 m thick fault zone between depths of about 4179–4184 m and a 1 m thick shear zone between 4180 m and 4181 m suggesting the actual location of the fault plane. This fault plane was clearly captured in the PANSAC fracture model as shown in Fig. 4 where the fitted plane has the highest association with seismic points (293 points, see Xu and Dowd (2014)). It is also interesting to note that the PANSAC statistical analysis indicates 5 m as the bandwidth of the variation in fracture tortuosity, which would be equivalent to the width of a fault plane. Fig. 5

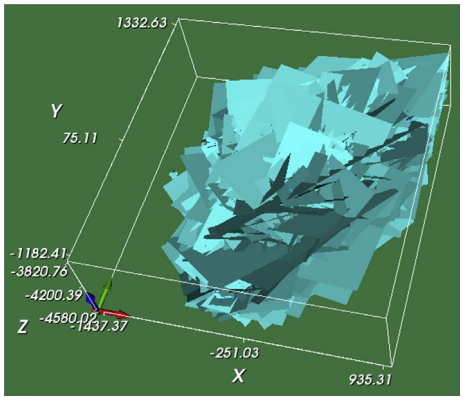

Fig. 3. Habanero fracture model generated by the PANSAC algorithm.

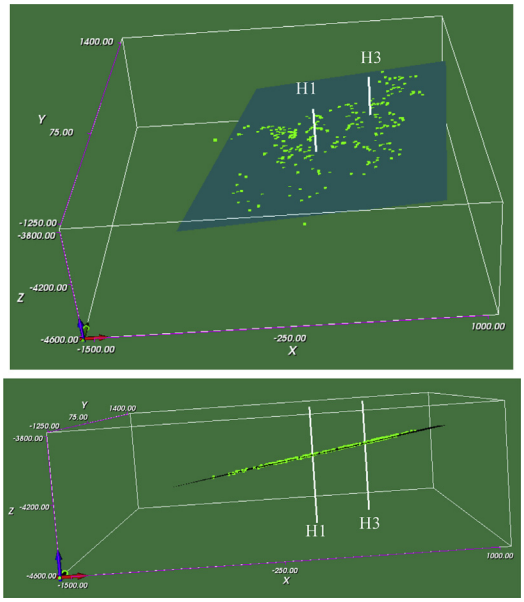

Fig. 4. The major faults captured by the PANSAC model.

shows the eight most significant fractures fitted to the Habanero reservoir; these fractures have the eight highest numbers of associated seismic points. Clearly the trend of fracture propagation, dipping slightly to the southwest as evident from the seismic point cloud, is captured in the model.

Conditional fracture models, such as those discussed above, are essential for realistic modelling of fluid flow and heat transfer in the reservoir. Although the major fault connects all wells directly, other fractures are equally, if not more, important for the geothermal fluid flow, particularly for heat extraction. This is confirmed by the tracer test described above which suggests the major flow paths between H1 and H3 may not necessarily be only along the major fault connecting the two wells; a significant portion of the flow will

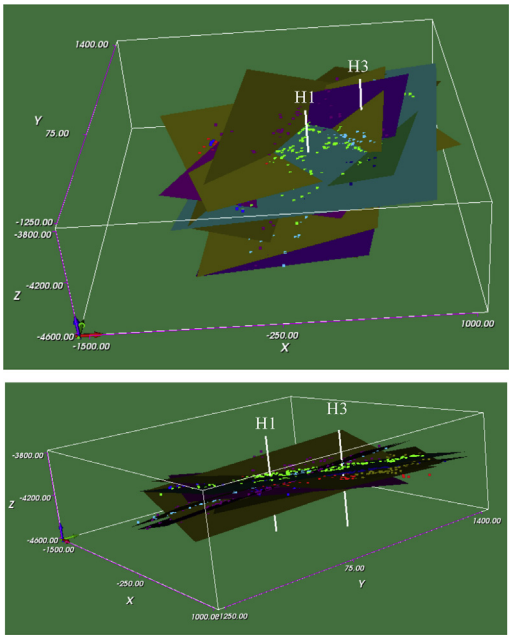

Fig. 5. The eight most significant fractures fitted to the Habanero seismic data.

be through other tortuous paths connecting the two wells. Early fluid flow and heat transfer models for this reservoir are largely based on an oversimplified single fracture model representing the major fault (Vörös and Weidler, 2006; Vörös and Rothert, 2009). Recent models are more realistic as they address the complexity of the fracture network in the reservoir either by using the MINC concept (Pruess and Narasimhan, 1985) implemented in TOUGH2 (Pruess et al., 1999) to model the fracture network (Geodynamics, 2014) or by using a fracture model such as that discussed above (Xu et al., 2015). For example, a connectivity analysis (Xu et al., 2012) of the fracture model displayed in Fig. 2 shows that there is a total of 27,293 possible connection channels through the fracture network between the two wells (H1 and H3). These connection paths are derived using the shortest path algorithm while considering all possible paths from a fracture intersection trace to the two wells.

In this connectivity analysis (Fig. 6), H1 is clearly well-connected to the surrounding rocks through the fracture model, which is expected because the fracture stimulation originates at this well. The much lower connection between H3 and the surrounding rocks is also expected as H3 does not contribute to the 2003 fracture stimulation on which this fracture model is based. Once the connection paths are derived, simulation of flow within the reservoir can proceed and one of the simplest approaches is to use the equivalent pipe network model which can significantly reduce the computational cost for large-scale projects (Dershowitz and Fidelibus, 1999; Xu et al., 2014). Fig. 7a shows the corresponding flow model of the reservoir based on this approach. For heat extraction, we have recently developed a simplified heat transfer (between fluid and rock) approach, the effectiveness of which has been demonstrated for large-scale and long time-span modelling (Xu et al., 2015). Fig. 7b shows the simulated temperature distribution within the Habanero reservoir after 20 years of heat production based on the fracture network model shown in Fig. 2.

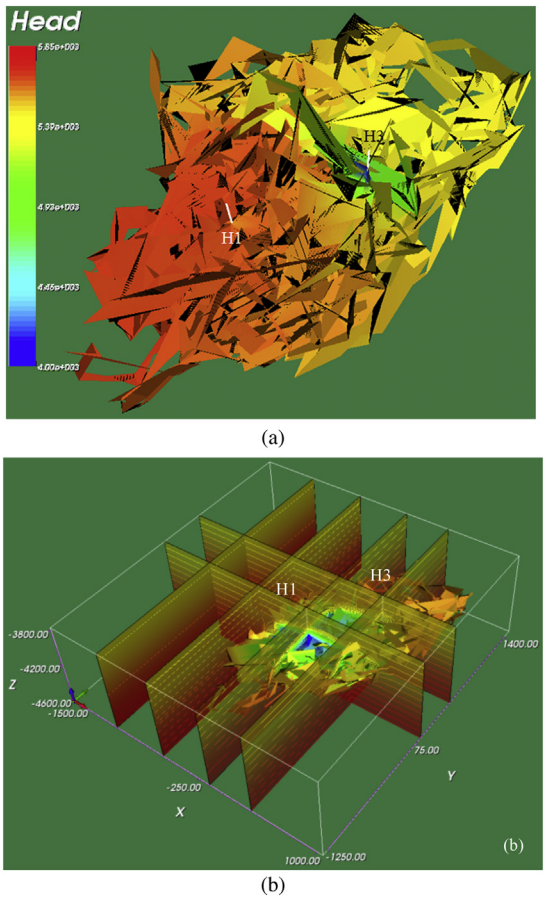

Fig. 7. Reservoir flow (a) and temperature (b) models of H1–H3 doublet.

5. Capacity for carbon sequestration of the Habanero geothermal field

The geothermal power produced from a geothermal reservoir depends on many variables. From the perspective of flow, the major factors are the flow rate (which, in turn, depends on fluid density and viscosity), the specific heat of the fluid and the heat transfer coefficient between the fluid and the rock. The geothermal power generation of the H1–H3 doublet has been modelled using different flow rates (Vörös and Rothert, 2009; Xu et al., 2015). Xu et al. (2015), using a flow rate of 35 L/s, modelled the production temperature and the geothermal power generated from the doublet over a 20-year production period as shown in Fig. 8.

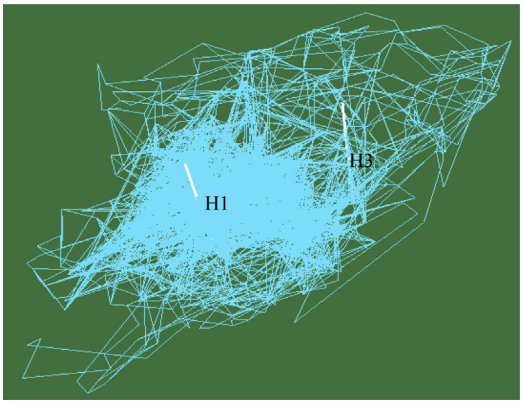

Fig. 6. Connection channels between H1 and H3.

These figures suggest a ratio of power to flow rate of 0.58 MW/L at the beginning of heat extraction. Other models give a ratio of 0.55 MW/L using a circulation rate of 15 L/s and a ratio of 0.57 MW/L using a flow rate of 25 L/s, even though they used different modelling approaches (Vörös and Rothert, 2009). The drops in production temperature and geothermal power after 20 years of continuous heat production are 50 °C and 7 MW using a flow rate of 35 L/s, 34 °C and 3.6 MW for a flow rate of 25 L/s, and 15.5 °C and 1 MW for a flow rate 15 L/s. As discussed above, the closed-loop circulation test of the H1–H4 doublet achieved a flow rate of 18.9 L/s and a production temperature of 215 °C at the end of the test, which is equivalent to geothermal power of approximately 10 MW. The power to flow rate ratio is therefore 0.53 MW/L and the models for the H1–H3 doublet give reasonably close answers. Based on these assessments, it is reasonable to use a conservative figure of 0.5 MW/L to approximate the geothermal power that could be generated from the Habanero reservoir. Note for the H1–H4 doublet circulation test, the electricity power generated is 1 MW, indicating a geothermal power utilisation efficiency of 10%, which is within the typical range of 6%–20% of geothermal power plants.

Pruess (2006) reported a detailed fluid flow and heat extraction analysis of the scenario of using $scCO_2$ as a working fluid for a hypothetical EGS reservoir. He used a traditional five-spot well pattern with the injection well located in the centre and the four production wells located at the four corners of a square over an area of 1 km^2. The reservoir temperature was 200 °C with a pressure of

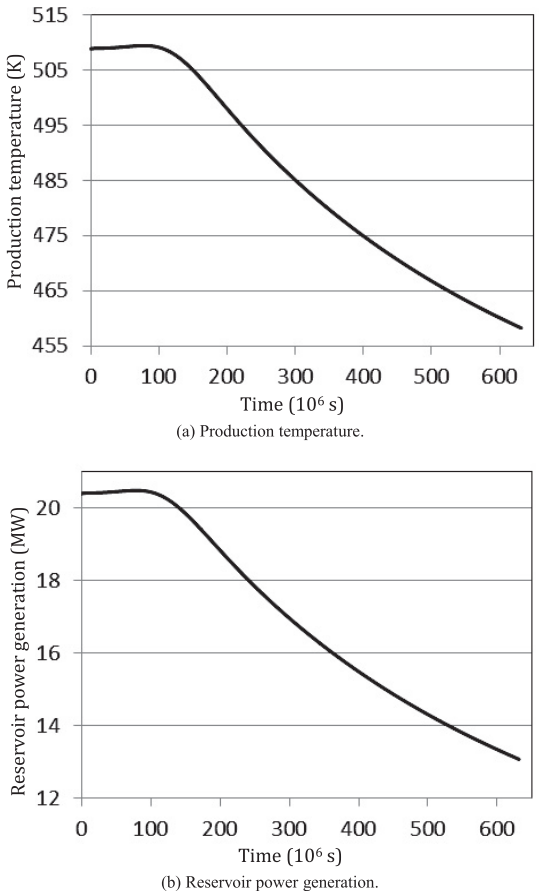

Fig. 8. Changes of production temperature and reservoir power generation with time.

50 MPa. The injection pressure was 51 MPa at a temperature of 20 °C and a production pressure of 49 MPa. The formation thickness modelled was 305 m. Fractures in the EGS reservoir were modelled with three orthogonal fracture sets with 50 m spacing and the matrix blocks were assumed to be impermeable and were sub-gridded into five continua using the multiple interacting continua (MINC) approach. The TOUGH2 code was used for the analysis.

From the simulation results, Pruess (2006) concluded that using $scCO_2$ instead of water as the working fluid and under the same operating conditions, the mass flow rate increases by a factor of 3.7 initially and rises to 4.7 after 36 years of production due to the lower viscosity of $scCO_2$ and the extra buoyancy force; the heat extraction rate (or geothermal power generated) increases by about 1.5 times initially, gradually rises to a maximum ratio of 1.7 times in about 16 years and then gradually decreases to about 1.4 times after 36 years of production. For the cases examined, when water is used as the working fluid, the flow rate is 80 kg/s, the geothermal power extracted is 60 MW and hence the power to flow rate ratio is 0.75 MW/L. But when $scCO_2$ is used, the flow rate is 300 kg/s, the heat extraction rate is 92 MW and the ratio is 0.31 MW/kg, or 0.18 MW/L using a fluid density of 580 kg/m^3 for $scCO_2$, which is about 24% of that when water is used per volume of fluid passing through the reservoir. Based on these assessments, it is reasonable to assume, for the Habanero reservoir, that if $scCO_2$ is used as the working fluid, the flow rate would be increased by at least 3.5 times and the heat extraction would be increased by at least 1.5 times. For example, if $scCO_2$ is used for the H1–H4 doublet in current conditions, the flow rate would be 66 kg/s and the geothermal power extracted would be 15 MW.

It is widely acknowledged that some of the fluid circulation in an EGS reservoir will be lost to the surrounding formations. This fluid loss is undesirable if the working fluid is water, but is an added advantage if $scCO_2$ is used as the CO_2 lost in circulation will be permanently stored in these formations. There are various mechanisms by which fluid loss can occur, as discussed in previous sections, but one of the major losses is by diffusion through the pores in the rock matrix, which is also considered to be one of the safest means of geological storage of CO_2. The rate loss to the pores is a function of many variables in the EGS, i.e.

$$Q = f(A_1, A_2, F, P_r, P_\infty, T, k, \varphi, \rho, \nu, s, t, \ldots) \quad (2)$$

where A_1 is the area of major flow paths and A_2 is the contact area between the fluid, both of which, in turn, depend on the fracture model F within the reservoir and its connectivity; P_r is the reservoir pressure and P_∞ is the background pore pressure; T is the reservoir temperature which in general significantly influences the hydrodynamic properties of the fluid; k and φ are the permeability and the porosity of the rock matrix, respectively, which largely dictate the flow rate within the rock matrix and, together with the saturation status s of the pores with other species, determine the total capacity available; ρ and ν are the density and viscosity of the fluid, respectively, which affect the flow characteristics; and t is the time as the loss rate is expected to be higher initially and then gradually reduce to zero (e.g. the fluid loss in the Fenton Hill Phase I system reduces to around 1% after 75 days of fluid circulation, see Brown et al. (2012)) when all possible spaces surrounding the reservoir are fully saturated in the case of a confined reservoir. A_1 and A_2 are two critical factors in this relationship as all fluid loss has to occur through this fluid-rock interaction area. These areas can be estimated once the conditional fracture model F, such as the one discussed above, has been derived. Note that A_2 includes the total area of all the fractures within the reservoir even if they do not participate in transporting the geothermal fluid for heat production. These fractures are also expected to be pressured in the heat extraction process and will therefore participate in dissipating the fluid into the rock matrix. This area is directly related to the fracture density $P32$ and a rough estimate for the Habanero reservoir of 0.3 was given in Xu and Dowd (2014) based on the PANSAC fracture model.

The derivation of the function Q is difficult unless significant simplifications are introduced. For example, if a single fracture model is used, the relationship can be derived assuming a Darcy flow. But oversimplification may degrade or eliminate the effects of the major mechanisms that govern the sequestration process, e.g. the fluid-rock intersection network. Experience from other EGS projects can at least provide a rough numerical approximation of the potential fluid loss during EGS heat extraction. The circulation test in the Fenton Hill Phase II system indicated a fluid loss as high as 17% initially followed by a gradual reduction to around 7% (Brown et al., 2012). As the Habanero reservoir is over-pressurised, it is possible to maintain the production rate at the injection rate for a short period of time, as was done in the closed-loop tests between H1 and H3 in 2005 and H1 and H4 in 2012. However, this operational arrangement does not mean there is no loss of the injection fluid to the surrounding rock mass and all injected fluid is fully returned. In fact, significant mud losses during drilling of the Habanero wells and the loss of tracers during the two tracer tests (H1–H3 in 2008 and H1–H4 in 2013) indicate that a significant amount of injected fluid is lost to the surrounding rock mass. Based on the figures obtained from the Fenton Hill project, Pruess (2006) suggested 5% as a reasonable estimate of the fluid loss when $scCO_2$ is used as the working fluid to drive EGS heat extraction. This figure has since been used often in the literature (e.g. Frank et al., 2012).

For the H1–H4 operation in current conditions, the fluid circulation requirement is approximately 44 kg/s of $scCO_2$ per MW of electric power produced, which is about twice the estimate of 21.8 kg/s used in Pruess (2006). However, it must be noted that in Pruess (2006), the overall geothermal energy utilisation efficiency used (including mechanical work efficiency and heat exchange efficiency) was 0.17, compared with 0.1 for the Habanero pilot plant output. If 0.17 is used instead of 0.1 for the utilisation efficiency, the fluid circulation requirement for the Habanero reservoir would be reduced to 25.9 kg/s of $scCO_2$ per MW of electric power, close to the figure given in Pruess (2006). Based on the suggested fluid loss figure and the actual pilot plant operation data for the H1–H4 doublet, the CO_2 losses would be around 2 kg/s per MW of electric power generated, again about twice the figure suggested by Pruess (2006). This would amount to around 63,000 t of CO_2 being sequestered per year per MW of electric power produced. For the doublet, a total of 94,500 t of CO_2 per year could be sequestered as the electric power produced is expected to be 1.5 MW if $scCO_2$ is used.

Geodynamics has now moved to the next phase in the potential commercial exploitation of the Habanero geothermal field. In the Geodynamics Field Development Plan (FDP, Geodynamics, 2014), the base project consists of six wells with a total production rate of 105 kg/s at a temperature of 220 °C yielding geothermal power of 57 MW. The nominal electric power is 7.5 MW using the new Organic Rankine Cycle (ORC) plant technology with an overall utilisation efficiency of around 13%. Using the ratios discussed above, if $scCO_2$ is used as the working fluid for the base project under the same conditions, the production rate would be 368 kg/s and the electric power 11 MW assuming the same overall utilisation efficiency. For the base project, 33 kg/s of $scCO_2$ per MW of electric power produced is needed for the circulation. Based on 5% fluid loss, this is equivalent to 52,000 t of CO_2 being sequestered per year per MW of electricity produced. For the entire base project, a total of 572,000 t of CO_2 per year could be stored. The base project covers approximately 2 $km^2 \times 500$ m with a six-spot well pattern. Compared with Pruess' modelling results, the total sequestration figure is relatively small as Pruess' simulation suggests a sequestration of around 404,000 t of CO_2 per year with an EGS reservoir covering 1 $km^2 \times 308$ m with a five-spot well pattern. Nevertheless, the 572,000 t potential CO_2 sequestration per year may over-estimate the storage capacity of the Habanero field (the reservoir plus the surrounding area) and it seems an unrealistically high capacity compared with several past and current CO_2 sequestration projects (Li et al., 2013a; ACCA21, 2014; Lv et al., 2015), particularly given the fact that the key purpose of a CO_2-EGS is for energy production and CO_2 sequestration is only a by-product. The porosity of the Habanero reservoir was estimated to be 1.4% for stimulated fractures and 0.36% for the damaged area based on history matching of the most recent H1–H4 tracer test. The porosity of the intact rock matrix was estimated to be 0.3%. Using 0.3% and assuming all voids are fully filled with CO_2, 572,000 t of CO_2 would cover a total reservoir volume of 3.29×10^8 m^3, equivalent to a cuboid of 690 m side length. Using an upper value of 10^{-3} mD as the permeability for the granite matrix (Bundschuh and Suárez-Arriaga, 2010) and a reservoir pressure of 100 MPa, according to Darcy's law, it would be impossible for CO_2 to travel a distance of even 100 m within one year even if a 100 MPa/m pressure gradient is assumed throughout the domain. On the other hand, it could be argued that the majority of fluid loss is to the stimulation damaged zone which has directional permeability in the east-west, north-south and vertical directions of 29 mD, 58 mD and 10 mD, respectively, estimated from the history matching of tracer and circulation test data. These permeability figures are several orders of magnitude higher than that of the rock matrix, for which Geodynamics suggested a figure of 10^{-7} mD (Geodynamics, 2014). Using 0.36% porosity for the damaged zone with a bandwidth of 5 m, the base project area of 2 km^2 and a vertical extent of 500 m (i.e. total reservoir volume of 1×10^9 m^3), 572,000 t of CO_2 stored only in the damaged zone would suggest a total stimulated fracture area of 5.5×10^7 m^2 which gives a value of 0.055 for fracture density $P32$. This value is modest and certainly quite possible but there is an obvious issue for the long-term storage capacity of the damaged zone. The total volume of the damaged zone is more or less fixed after stimulation and the zone will contribute to fluid transport during the production process. Its storage capacity will diminish once its void space is fully saturated. Even if a $P32$ value of 0.3 is used, the storage capacity of the damaged zone would reduce to zero by about 5.5 years with a constant sequestration rate of 572,000 t/a (in reality it would be a higher sequestration rate initially followed by a gradual reduction to zero). These figures suggest that the major mechanisms of CO_2 sequestration are the storage in the stimulation damaged zone followed by diffusion into the pores of the rock matrix. The 5% of fluid loss in a CO_2-EGS may be an over-estimate of the long-term storage capacity of EGS reservoirs. We have not considered leakage in this study because it is not a critical issue for the Habanero field given the significant depth of the reservoir (>4 km) and the geological setting. The injection tests conducted on the Habanero wells indicate that Habanero is a confined reservoir tightly sealed from the overlaying sediments. Table 2 provides a summary of the figures used in this comparative study.

Another factor to be considered is that, in the case of the Habanero field, the reservoir is over-pressurised, possibly fully

Table 2
Comparative study of the power generation and CO_2 storage capacity of CO_2-EGS.

Model	Model size ($km^2 \times m$)	Temperature (°C)	Water/brine as the working fluid				Comparisons	
			Flow rate (A) (kg s^{-1})	Geothermal power (B) (MW)	Power to flow ratio (=B/A) (MW kg^{-1} s^{-1})	Electrical power (MW)	Flow rate ratio (=C/A)	Geothermal power ratio (=D/B)
Pruess's model	1 × 305	200 (reservoir)	80	60	0.75		3.75	1.53
H1–H3 doublet	~1.5 × 500	225/231/236 (production)	15/25/35	8.2/14.3/20.3	0.55/0.57/0.58			
H1–H4 doublet	~1.5 × 500	215 (production)	18.9	10	0.53	1	3.5	1.5
Habanero FDP	2 × 500	220 (production)	105	57		7.5	3.5	1.5

Model	$scCO_2$ as the working fluid					CO_2 sequestration capacity		Reference
	Flow rate (C) (kg s^{-1})	Geothermal power (D) (MW)	Power to flow ratio (=D/C) (MW kg^{-1} s^{-1})	Electrical power, $scCO_2$ (MW)	Fluid requirement (kg s^{-1} MW^{-1})	Fluid loss (%)	Sequestration capacity (t a^{-1})	
Pruess's model	300	92	0.31	15.64	21.8 @ 17% utilisation	5	404,000	Pruess (2006)
H1–H3 doublet								Vörös and Rothert (2009); Xu et al. (2015)
H1–H4 doublet	66	15	0.23	1.5	44 @ 10% utilisation	5	94,500	Geodynamics (2014)
Habanero FDP	368	85.5	0.23	11	33 @ 13% utilisation	5	572,000	Geodynamics (2014)

saturated with brine. If $scCO_2$ is to be used as the working fluid, reservoir de-pressurising (e.g. using open flow) may be necessary which would then be followed by the displacement of water by $scCO_2$. There has been a considerable amount of research done in the latter area and a detailed discussion is beyond the scope of this paper. Interested readers are referred to Li et al. (2013b, 2014). One potential issue is when CO_2 is mixed with water it can form highly corrosive acidic flow which may cause considerable dissolution/precipitation problems in the reservoir and corrosion/scaling in the pipes. Of course, there is an added advantage of this scenario as the produced brine can be desalinated to produce fresh water (Li et al., 2015a), which is a scarce resource in the Habanero region.

6. Conclusions

This paper assesses the CO_2 sequestration potential of the Habanero geothermal field in the Cooper Basin of South Australia if $scCO_2$ is used as the working fluid to generate heat production. The existing H1–H4 doublet is estimated to be capable of storing 94,500 t of CO_2 per year based on the conditions prevailing during the pilot plant demonstration operation. The next stage base project with a six-spot well pattern is estimated to be capable of storing 572,000 t of CO_2 per year. These figures are calculated on the assumption of 5% fluid loss normally used in CO_2-EGS. The analysis of the sequestration capacity of the Habanero field suggests that the major CO_2 sequestration mechanisms are the storage in the stimulation damaged zone and diffusion into the rock matrix; 5% of storage capacity might be an over-estimate of the long-term percentage of fluid that is lost in circulation and mineral trapping in a typical HDR EGS such as the one in the Habanero field.

Conflict of interest

The authors wish to confirm that there are no known conflicts of interest associated with this publication and there has been no significant financial support for this work that could have influenced its outcome.

Acknowledgements

The work described here was funded by Australian Research Council Discovery Project (Grant No. DP110104766). We thank Geodynamics Limited for allowing access to the microseismic data and some internal technical reports. Dr. Qi Li acknowledges financial support from the China Australia Geological Storage of CO_2 Project (CAGS) and Australia–China Young Researchers Exchange Program 2012.

References

ACCA21. An assessment report on CO_2 utilization technologies in China. Beijing: Science Press; 2014 (in Chinese).
Albert G, Nicolas C, Xavier G, Bernd M, Bernard S, Julia S. Status of the Soultz geothermal project during exploitation between 2010 and 2012. In: Proceedings of the 37th Workshop on Geothermal Reservoir Engineering. Stanford, California; 2012.
Baisch S, Weidler R, Vörös R, Wyborn D, de Graaf L. Induced seismicity during the stimulation of a geothermal HFR reservoir in the Cooper Basin, Australia. Bulletin of the Seismological Society of America 2006;96(6):2242–56.
Bear J, Cheng AD. Modeling groundwater flow and contaminant transport. Springer; 2010.
BESTEC. http://www.bestec-for-nature.com/j_bestec/index.php/en/projects/landau; 2012.
Bundschuh J, Suárez-Arriaga M. Introduction to the numerical modeling of groundwater and geothermal systems: fundamentals of mass, energy and solute transport in poroelastic rocks. Leiden, Netherlands: CRC Press; 2010.
Brown DW, Duchane DV, Heiken G, Hriscu VT. Mining the Earth's heat: hot dry rock geothermal energy. Berlin Heidelberg: Springer-Verlag; 2012.
Brown DW. A hot dry rock geothermal energy concept utilising supercritical CO_2 instead of water. In: Proceedings of the 25th Workshop on Geothermal Reservoir Engineering. Stanford, California; 2000.
Duchane D, Brown D. Hot dry rock (HDR) geothermal energy research and development at Fenton Hill, New Mexico. GHC Bulletin 2002:13–9.
Dershowitz WS, Fidelibus C. Derivation of equivalent pipe network analogues for three-dimensional discrete fracture networks by boundary element method. Water Resources Research 1999;35(9):2685–91.
Fadakar AF, Dowd PA, Xu C. The RANSAC method for generating fracture networks from micro-seismic event data. Mathematical Geosciences 2013;45(2):207–24.
Frank ED, Sullivan JL, Wang MQ. Life cycle analysis of geothermal power generation with supercritical carbon dioxide. Environmental Research Letters 2012;7:034030.
Geodynamics. Hananero geothermal project field development plan. Geodynamics Ltd.; 2014. Document No. COM-FN-OT-PLN-01166.
Huisingh D, Zhang Z, Moore JC, Qiao Q, Li Q. Recent advances in carbon emissions reduction: policies, technologies, monitoring, assessment and modeling. Journal of Cleaner Production 2015. http://dx.doi.org/10.1016/j.jclepro.2015.04.098.
Kaieda H, Ito H, Kiho K, Suzuki K, Suenaga H, Shin K. Review of the Ogachi HDR project in Japan. In: Proceedings of the World Geothermal Congress 2005. Antalya, Turkey; 2005.
Li Q, Wei Y, Liu G, Jing M, Zhang M, Fei W, Li X. Feasibility of the combination of CO_2 geological storage and saline water development in sedimentary basins of China. Energy Procedia 2013b;37:4511–7.
Li Q, Wei YN, Liu G, Lin Q. Combination of CO_2 geological storage with deep saline water recovery in western China: insights from numerical analyses. Applied Energy 2014;116:101–10.
Li Q, Wei YN, Liu G, Shi H. CO_2-EWR: a cleaner solution for coal chemical industry in China. Journal of Cleaner Production 2015. http://dx.doi.org/10.1016/j.jclepro.2014.09.073.
Li Q, Chen ZA, Zhang JT, Liu LC, Li XC, Jia L. Positioning and revision of CCUS technology development in China. International Journal of Greenhouse Gas Control 2015. http://dx.doi.org/10.1016/j.ijggc.2015.02.024.
Li Q, Liu G, Liu X, Li X. Application of a health, safety, and environmental screening and ranking framework to the Shenhua CCS project. International Journal of Greenhouse Gas Control 2013a;17:504–14.
Lv GZ, Li Q, Wang S, Li X. Key techniques of reservoir engineering and injection-production process for CO_2 flooding in China's SINOPEC Shengli Oilfield. Journal of CO_2 Utilization 2015. http://dx.doi.org/10.1016/j.jcou.2014.12.007.
Matsunaga I, Niitsuma H, Oikawa Y. Review of the HDR development at Hijiori Site, Japan. In: Proceedings of the World Geothermal Congress 2005. Antalya, Turkey; 2005.
Massachusetts Institute of Technology (MIT). The future of geothermal energy. Assessment by an MIT-led interdisciplinary panel. 2006. http://www.eere.energy.gov/geothermal/egs_technology.html.
Mardia KV, Nyirongo VB, Walder AN, Xu C, Dowd PA, Fowell RJ, Kent JT. Markov Chain Monte Carlo implementation of rock fracture modelling. Mathematical Geology 2007;39:355–81.
Manrique E, Thomas C, Ravikiran R, Izadi M, Lantz M, Romero J, Alvarado V. EOR: current status and opportunities. SPE 130113. Society of Petroleum Engineers; 2010.
Metz B, Davidson O, de Coninck H, Loos M, Meyer L. IPCC special report on carbon dioxide capture and storage. Cambridge, UK: Cambridge University Press; 2005.
Oikawa Y, Tenma N, Yamaguchi T, Karasawa H, Egawa Y, Yamauchi T. Heat extraction experiment at Hijiori test site. In: Proceedings of the 26th Workshop on Geothermal Reservoir Engineering, Stanford, California; 2001. SGP-TR-168.
Parker R. The rosemanowes HDR project 1983–1991. Geothermics 1999;28(4–5):603–15.
Pruess K, Narasimhan T. A practical method for modeling fluid and heat flow in fractured porous media. Society of Petroleum Engineers Journal 1985;1:14–26.
Pruess K, Oldenburg C, Moridis G. TOUGH2 user's guide, Version 2.0. LBNL-43134. Ernest Orlando Lawrence Berkeley National Laboratory; 1999.
Pruess K. Enhanced geothermal system (EGS) using CO_2 as working fluid–A novel approach for generating renewable energy with simultaneous sequestration of carbon. Geothermics 2006;35(4):351–67.
Seifollahi S, Dowd PA, Xu C, Fadakar AF. A spatial clustering approach for stochastic fracture network modelling. Rock Mechanics and Rock Engineering 2014a;47(4):1225–35.
Seifollahi S, Dowd PA, Xu C. An enhanced stochastic optimization in fracture network modelling conditional on seismic events. Computers and Geotechnics 2014b;61:85–95.
Selvadurai APS, Boulon MJ, Nguyen TS. The permeability of an intact granite. Pure and Applied Geophysics 2005;162(2):373–407.
Tenzer H. Development of hot dry rock technology. GHC Bulletin 2001:14–22.
Vörös R, Weidler R. Numerical thermo-hydraulic simulation of a large scale power production in the Cooper Basin. Geodynamics Ltd.; 2006. Technical Report GDY018.
Vörös R, Rothert E. Simulation of the thermal drawdown for a circulation between Habanero #1–Habanero #3. Geodynamics Ltd.; 2009. Technical Report GDY028.
Weidler R. The Cooper Basin HFR project 2003/3004: findings, achievements and implications. Geodynamics Ltd.; 2005.
Wyborn D. Enhanced geothermal systems (EGS) development–10 years experience in the Innamincka granite, Australia. In: The 34th International Geological Congress. Brisbane, Australia; 2012.

Xie H, Li X, Fang Z, Wang Y, Li Q, Shi L, Bai B, Wei N, Hou Z. Carbon geological utilization and storage in China: current status and perspectives. Acta Geotechnica 2014;9(1):7–27.
Xu C, Dowd PA, Mohais R. Connectivity analysis of the Habanero enhanced geothermal system. In: Proceedings of the 2012 Stanford Geothermal Workshop. Stanford, California; 2012. SGP-TR-194.
Xu C, Dowd PA, Wyborn D. Optimisation of a stochastic rock fracture model using Markov Chain Monte Carlo simulation. Mining Technology 2013;122(3):153–8.
Xu C, Dowd PA. Stochastic fracture propagation modelling for enhanced geothermal systems. Mathematical Geosciences 2014;46(6):665–90.
Xu C, Dowd PA, Tian ZF. A simplified coupled hydro-thermal model for enhanced geothermal systems. Applied Energy 2015;140:135–45.
Xu C, Fidelibus C, Dowd PA. Realistic pipe models for flow modelling in discrete fracture networks. In: Proceedings of the First International Discrete Fracture Network Engineering Conference, Vancouver, Canada; 2014. Paper No. 132.

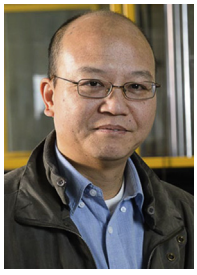

A/Prof. **Chaoshui Xu** is a founding member of the Mining Engineering programme at University of Adelaide. He has over thirty years of experience working for mining academic institutions and the industry. His broad research interests cover many areas including geostatistics, mineral resource evaluation, risk assessment of mining project, optimal mine design, rock fracture mechanics, stochastic rock fracture modelling, fluid flow and heat transfer in porous or fractured rock.

Peter Dowd is Professor of Mining Engineering at the University of Adelaide and Executive Director of Mining Education Australia. He is a Fellow of the Royal Academy of Engineering and a Fellow of the Australian Academy of Technological Sciences and Engineering. His research interests cover geostatistics, quantitative geology mine design and optimisation, and the stochastic modelling and simulation of fracture networks in rock masses.

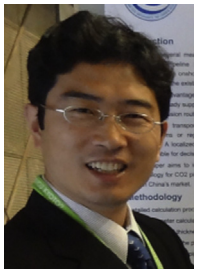

Qi Li (1995 BSc; 1998 MSc; 2004 PhD) is now Research Scientist and Professor at Institute of Rock and Soil Mechanics (IRSM), Chinese Academy of Sciences. He is a geoscientist with expertise in the fields of carbon dioxide geosequestration and acid gas injection. His research is focused on understanding and using laboratory and numerical tools to design novel subsurface disposal processes and related monitoring systems on different temporal and spatial scales.